Boundary crisis in quasiperiodically forced systems

Hinke Osinga[1,*] and Ulrike Feudel[2,†]

[1] *Control and Dynamical Systems, California Institute of Technology 107-81, Pasadena, CA 91125, U.S.A.*

[2] *Institut für Physik, Universität Potsdam, PF 601553, D-14415 Potsdam, Germany*

Abstract

We study boundary crisis in quasiperiodically forced dissipative systems using the Hénon map as a characteristic example. The crisis is due to a homoclinic tangency of the stable and unstable manifolds of an accessible invariant circle of saddle type on the basin boundary of the attractor. Numerical evidence shows that the saddle that induces the boundary crisis can change due to the quasiperiodic forcing. This implies the existence of codimension-two *double crisis vertices* where a curve of boundary crisis and a curve of interior crisis meet. We argue that bifurcation points of higher codimension must exist in the full parameter space.

PACS-numbers: 05.45.-a

Keywords: boundary crisis, homoclinic tangency, double crisis vertex

*Corresponding author: hinke@cds.caltech.edu, +1 626 395-6943 / 796-8914 (fax)
†ulrike@agnld.uni-potsdam.de

1 Introduction

Attractors, and in particular chaotic attractors have long been the focus of attention. Of special interest are the mechanisms that induce their appearance and disappearance. The most dramatic such transitions are so-called crises [11] in which an attractor undergoes a sudden change. Two different kinds of crises are distinguished. A chaotic attractor can suddenly disappear due to a boundary crisis or change in size due to an interior crisis. Typically, studies have been focused on two-dimensional dissipative maps, where attention was paid to transient or intermittent dynamics after a boundary crisis or interior crisis, respectively [10, 13]. Other investigations are devoted to curves of boundary crisis in parameter space [9, 22].

In this paper we study the boundary crisis for a particular class of systems, namely quasiperiodically forced systems. Quasiperiodically forced systems are systems that are influenced by two external periodic signals with incommensurate frequencies. Theoretical studies of the behavior of such systems can be found in [2, 6, 8]. Experimental investigations of quasiperiodically forced systems include work with an electronic Josephson junction simulator [17], studies of three-frequency motion and transitions to chaos in an electron hole plasma [15], and demonstrating the existence of different types of attractors using a quasiperiodically forced magneto-elastic ribbon [7].

Most theoretical studies describe quasiperiodically forced systems by a map for which one coordinate behaves as a rotation by an irrational number. Variations of the parameters in the model cause changes in the dynamical behavior of the system, known as bifurcations at critical parameter values. Besides well-known bifurcations, for example saddle-node bifurcations for invariant curves [4], there exist new bifurcations related to the appearance of so-called strange nonchaotic attractors [20, 23, 24].

The boundary crisis for a quasiperiodically forced dissipative map is induced by a homoclinic bifurcation, where the stable and unstable manifolds of an invariant circle of saddle type on the basin boundary of the attractor become tangent. We call this invariant circle the *crisis circle*. Our investigation shows that under quasiperiodic forcing the crisis circle is not always the same circle, that is, for certain forcing amplitudes the homoclinic tangency of the manifolds of the crisis circle does not induce a boundary crisis, but a basin boundary metamorphosis, and another circle, with another period, becomes the crisis circle. We study this phenomenon in a two-parameter plane, where one parameter is the forcing amplitude and the other parameter is the strength of nonlinearity in the system. The homoclinic tangency happens along a smooth curve that corresponds to the boundary crisis, except for a finite segment where it induces a basin boundary metamorphosis changing the smoothness properties of the basin boundary of the attractor. This segment is bounded by a pair of *double crisis vertices*. At each vertex two additional curves meet, namely another boundary crisis curve with a different crisis circle, and a curve that represents an interior crisis where the size of the attractor changes suddenly.

The paper is organized as follows. In Sec. 2 we introduce the quasiperiodically forced Hénon map which we use as a paradigm to study the boundary crisis in quasiperiodically forced two-dimensional dissipative maps. We briefly recall the characteristics of boundary crisis in the standard Hénon map relevant for our further investigation (Sec. 3). Section 4 is devoted to the boundary crisis in two-dimensional dissipative maps under the influence of quasiperiodic forcing. We study in detail the standard boundary crisis (Subsec. 4.1) and the basin boundary metamorphosis (Subsec. 4.2), and we discuss the double crisis vertices in the two-dimensional parameter space (Subsec. 4.3). In the discussion (Sec. 5) we conjecture that in the full, three-dimensional parameter space *multiple crisis vertices* have to be expected.

2 The quasiperiodically forced Hénon map

The quasiperiodically forced Hénon map is introduced in [21] as

$$\left\{\begin{array}{lcl} \vartheta_{n+1} & = & \vartheta_n + \omega \pmod 1, \\ u_{n+1} & = & 1 + v_n - b u_n^2 + A\cos(2\pi\vartheta_n), \\ v_{n+1} & = & c u_n, \end{array}\right. \tag{1}$$

where $\omega = \frac{1}{2}(\sqrt{5}-1)$, the inverse of the golden mean, is fixed. We use this model as a characteristic example of a two-dimensional dissipative map with external quasiperiodic forcing. The equation for ϑ describes the quasiperiodic forcing, a rigid rotation by the irrational number ω. For $A = 0$, the two equations for u and v form the well-known Hénon map [16]. The determinant of the Jacobian matrix (both two- and three-dimensional) is constant and equal to $-c$, which controls the dissipativity of the map. We restrict our investigation to the case $c = 0.1$. With b in front of the nonlinearity we can control whether the attractor is chaotic or not. The parameter A models the amplitude of the forcing. With ω and c fixed we think of (1) as a two-parameter family with parameters A and b and study the boundary crisis only in this parameter plane.

In our numerical investigations it is important to distinguish between chaotic and nonchaotic attractors. We check this by calculating the Lyapunov exponents. The exponent that corresponds to the quasiperiodic forcing is always zero, so that only two Lyapunov exponents are relevant for the distinction between chaotic and nonchaotic motion. If one of those two exponents is positive, the attractor is chaotic. We also compute unstable invariant curves and their stable and unstable manifolds using the algorithms described in the Appendix.

3 Boundary crisis: the unforced case

Let us first give a brief introduction to boundary crisis in unforced maps by considering the Hénon map [16]

$$\begin{cases} u_{n+1} &= 1 + v_n - b\,u_n^2, \\ v_{n+1} &= c\,u_n, \end{cases} \tag{2}$$

with $c = 0.1$. According to [11], a boundary crisis is the collision of a chaotic attractor with an unstable fixed point or periodic orbit on its basin boundary. In the case of a two-dimensional dissipative map, e.g. the Hénon map with $|c| < 1$, the boundary crisis is induced by a homoclinic or heteroclinic tangency of stable and unstable manifolds [11]. There exists an attractor approximately for $b < 1.80324$. The basin of the attractor is bounded by the closure of the stable manifold $W^s(p_{\mathcal{B}})$ of a saddle point $p_{\mathcal{B}} = p_{\mathcal{B}}(b, c)$ on the basin boundary. One branch of the unstable manifold $W^u(p_{\mathcal{B}})$ of $p_{\mathcal{B}}$ goes to the attractor. Furthermore, if the attractor is chaotic, it is formed by the closure of the unstable manifold $W^u(p_{\mathcal{A}})$ of a saddle point $p_{\mathcal{A}} = p_{\mathcal{A}}(b, c)$ on the attractor; see Fig. 1(a) with $b = 1.6$. Note that the attractor is at the same time a subset of the closure of $W^u(p_{\mathcal{B}})$. The attractor collides with $p_{\mathcal{B}}$ for $b \approx 1.80324$ in a boundary crisis, and it has disappeared for $b > 1.80324$. Figure 1(b) shows $W^u(p_{\mathcal{A}})$ and $W^s(p_{\mathcal{B}})$ for $b = 1.80324$. The picture indicates that, for $b \approx 1.80324$, there is a heteroclinic tangency between the closures of $W^u(p_{\mathcal{A}})$ and $W^s(p_{\mathcal{B}})$. We remark that at this moment the attractor is also equal to the closure of one branch of $W^u(p_{\mathcal{B}})$, which means that, at the same

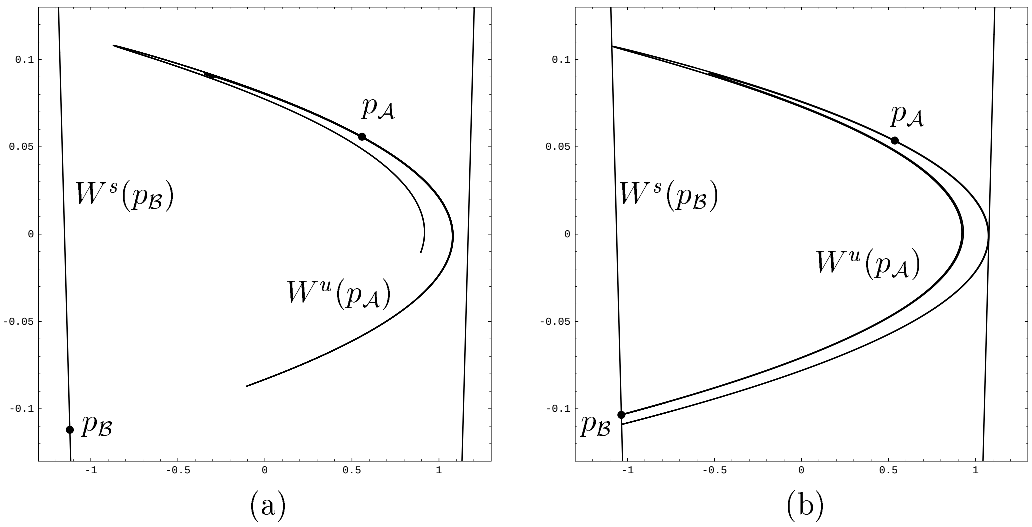

Figure 1: *Boundary crisis for the Hénon map with* $c = 0.1$. *Before the crisis, (a) with* $b = 1.6$, *the attractor is the closure of* $W^u(p_{\mathcal{A}})$, *and its basin boundary is the closure of* $W^s(p_{\mathcal{B}})$. *At the moment of crisis, (b) with* $b = 1.80324$, *the attractor is also equal to the closure of one branch of* $W^u(p_{\mathcal{B}})$.

time, there is a homoclinic tangency between the closures of the stable and unstable manifolds of $p_{\mathcal{B}}$.

The boundary crisis does not always involve the manifolds of the saddle points $p_{\mathcal{A}}$ and $p_{\mathcal{B}}$. For example, if we take $c = 0.6$, then the attractor persists after the homoclinic tangency of the closures of $W^s(p_{\mathcal{B}})$ and $W^u(p_{\mathcal{B}})$; see Fig. 2(a) with $b = 0.95$, where the stable and unstable manifolds of $p_{\mathcal{B}}$ are drawn together with the attractor. For clarity, we omitted $W^u(p_{\mathcal{A}})$, which also intersects $W^s(p_{\mathcal{B}})$. The attractor is now only a subset of the closure of $W^u(p_{\mathcal{A}})$, and it disappears after it collides with a period-six saddle on its basin boundary for $b \approx 0.96136$; see Fig. 2(b). After the homoclinic tangency of the closures of the manifolds of $p_{\mathcal{B}}$, the relative size of the basin of attraction shrinks a lot and the basin boundary, which is still the closure of $W^s(p_{\mathcal{B}})$, becomes fractal. This is known as a *basin boundary metamorphosis* [1, 12, 14]. Due to the homoclinic tangle, the point $p_{\mathcal{B}}$ is no longer accessible from the interior of the basin of attraction of the attractor. This means that $p_{\mathcal{B}}$ can no longer induce a boundary crisis. The closure of one branch of the unstable manifold of the period-six saddle is equal to the attractor

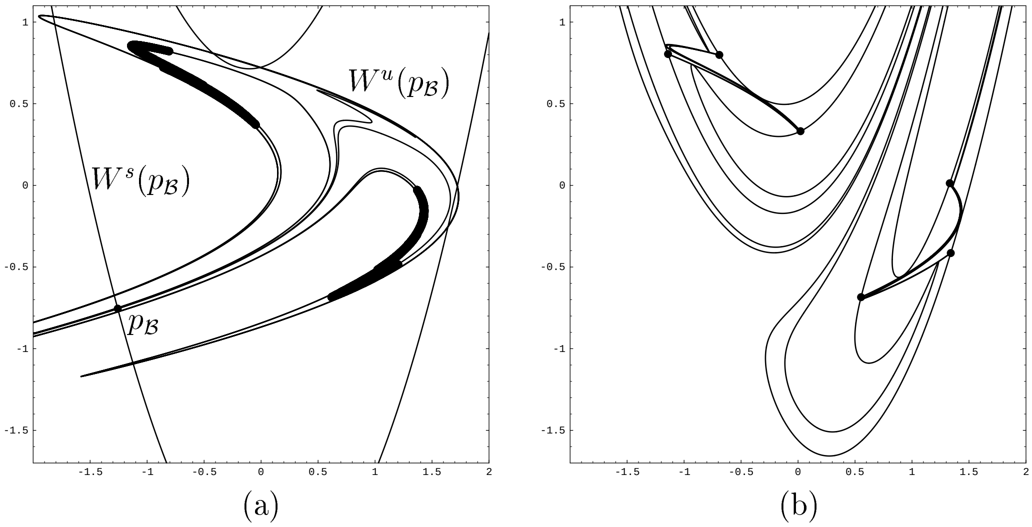

Figure 2: *Boundary crisis for the Hénon map with* $c = 0.6$*. The attractor persists after the homoclinic tangency of the closures of* $W^u(p_{\mathcal{B}})$ *and* $W^s(p_{\mathcal{B}})$*, (a) with* $b = 0.95$*. The boundary crisis is induced by the homoclinic tangency of the closures of the stable and unstable manifolds of a period-six saddle on the basin boundary, (b) with* $b = 0.96136$*.*

at the moment of tangency. This means that the boundary crisis can be identified with the homoclinic tangency of the manifolds of the period-six saddle. Hence, a homoclinic tangency of the manifolds of the saddle $p_{\mathcal{B}}$ induces a boundary crisis if the attractor, at the moment of tangency, is *equal* to the closure of one branch of $W^u(p_{\mathcal{B}})$. It induces a basin boundary metamorphosis if the attractor is only a *subset* of the closure of one branch of $W^u(p_{\mathcal{B}})$.

4 Boundary crisis: the forced case

Let us now consider the Hénon map with external quasiperiodic forcing (1) described in Sec. 2. The first (external) coordinate of this three-dimensional map is on the unit circle and behaves as a quasiperiodic rigid rotation. The unstable fixed point or periodic orbit involved in the boundary crisis now becomes an unstable invariant circle. It is already indicated in the conclusions

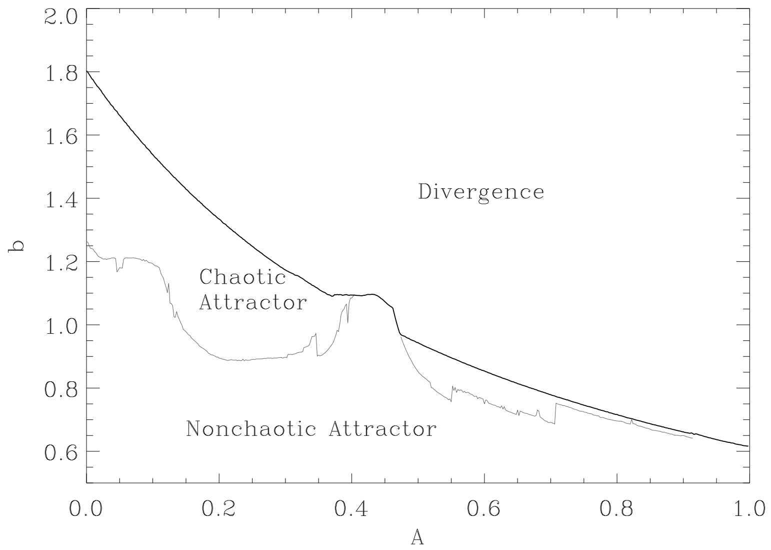

Figure 3: *A sketch of the bifurcation diagram for the quasiperiodically forced Hénon map. The curve of boundary crisis bounds the region where there is no attractor (Divergence).*

of [11] that the definition of a crisis may need to be extended. We define a boundary crisis as the collision of a chaotic attractor with an unstable (periodic) point or invariant (periodic) circle. Since our model is essentially the Hénon map times a rigid rotation, it seems natural to expect behavior very similar to the two-dimensional case without external forcing. However, we give numerical evidence that in open regions of parameter space the boundary crisis in a two-dimensional map with quasiperiodic forcing can be different from the corresponding crisis in the unforced map.

For each value of the forcing amplitude A there is exactly one value of b at which a boundary crisis takes place. These points form a curve in the (A, b)-parameter plane that is parametrized by A; see Fig. 3. Below this curve an attractor exists that may be chaotic or not. The other curve shown in Fig. 3 indicates where the attractor becomes chaotic for the first time. Windows within the chaotic parameter region, where the motion is again nonchaotic are not shown. The attractor may also consist of more than one piece. However, at the moment of boundary crisis, the attractor is always a single connected set. Let us now discuss in detail the transition

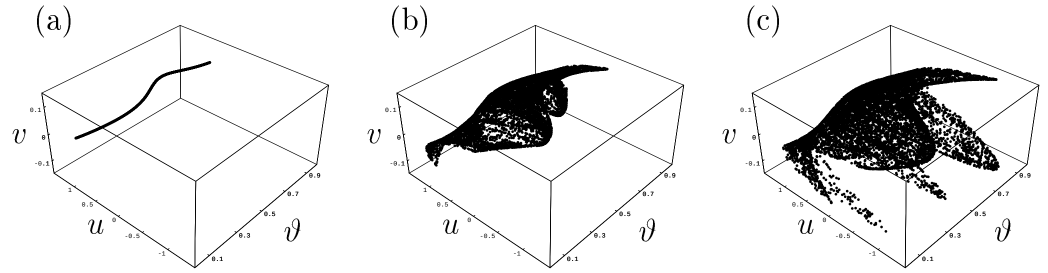

Figure 4: *For $A = 0.2$ fixed, the attractor changes from a smooth circle, (a) with $b = 0.5$, to a chaotic attractor, (b) with $b = 1.0$, and (c) with $b = 1.33$ just before the boundary crisis at $b \approx 1.334$.*

phenomena along the curve of boundary crisis; see also the animations at `http://www.cds.caltech.edu/~hinke/crisis`.

4.1 Standard boundary crisis

The unforced case with $A = 0$ is described in Sec. 3. When the forcing is switched on ($A \neq 0$), the saddle $p_{\mathcal{B}}$ in Fig. 1 becomes a circle $H_{\mathcal{B}} = H_{\mathcal{B}}(A, b)$ for (1) with two-dimensional stable and unstable manifolds. However, a cross-section with ϑ constant, for any $\vartheta \in \mathbb{R}/\mathbb{Z}$, looks like Fig. 1. Therefore, we expect that also for $A \approx 0$ the quasiperiodically forced Hénon map has a chaotic attractor that disappears in a boundary crisis induced by the homoclinic tangency of the stable and unstable manifolds of $H_{\mathcal{B}}$.

In fact, for almost all A-values the boundary crisis is due to a homoclinic tangency of the stable and unstable manifolds of $H_{\mathcal{B}}$. We illustrate this with numerical computations for $A = 0.2$ and varying b. For small b the attractor is a smooth invariant circle. There is a period-doubling bifurcation at $b \approx 0.6479$, after which the attractor consists of two pieces. For $b \approx 0.896$ the attractor becomes chaotic, and at $b \approx 0.8997$ the two pieces merge in what is called a *band merging bifurcation* [21, 5]. Now the attractor again consists of only one piece and it is chaotic. The attractor disappears in a boundary crisis for $b \approx 1.334$; see Fig. 4. For $A = 0.2$ and several values of b we computed an approximation of $H_{\mathcal{B}}$ and its stable and unstable manifolds. The closure of the two-dimensional stable manifold of $H_{\mathcal{B}}$ forms the basin boundary of the attractor, and one branch of its two-dimensional unstable manifold accumulates on the attractor. The results are shown in

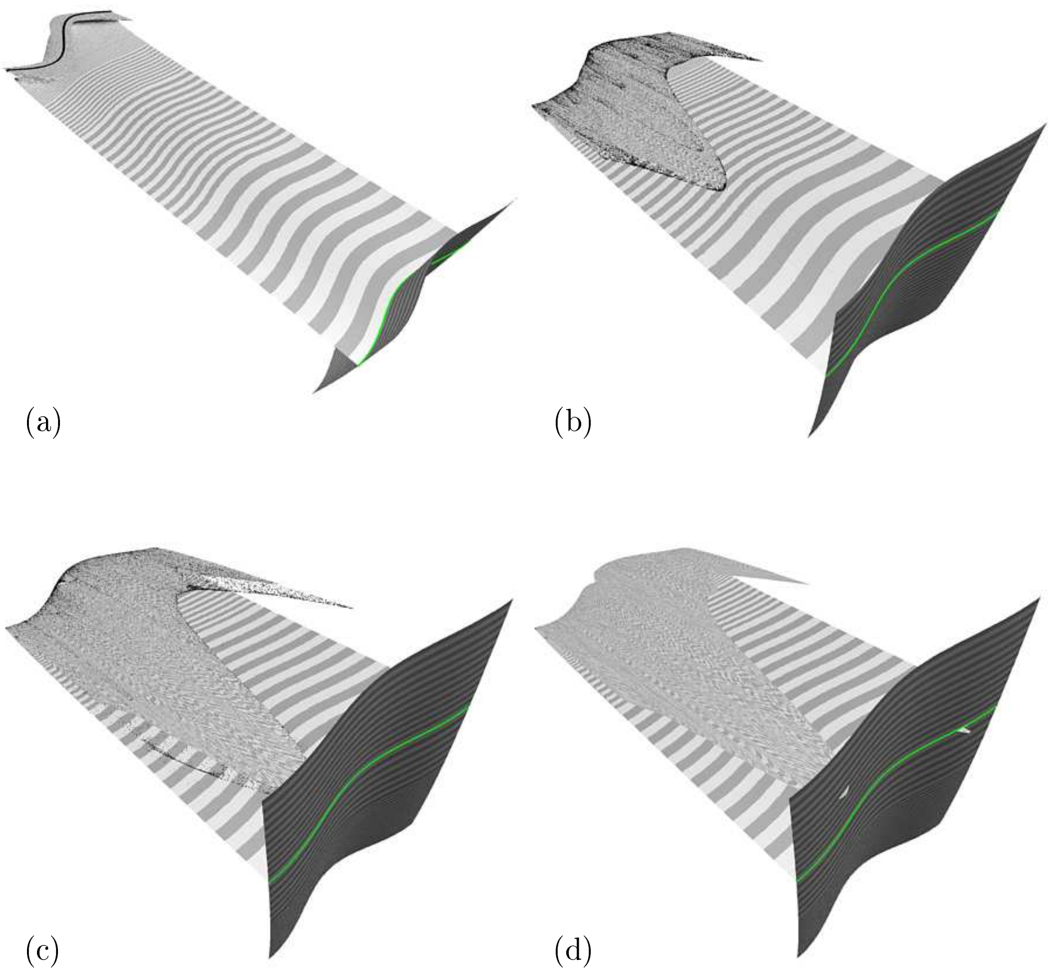

Figure 5: *For $A = 0.2$ fixed, the basin boundary of the attractor is equal to the closure of $W^s(H_{\mathcal{B}})$. One branch of $W^u(H_{\mathcal{B}})$ accumulates on the attractor; (a) with $b = 0.5$, (b) with $b = 1.0$. The attractor disappears in a boundary crisis for $b \approx 1.334$; (c) just before with $b = 1.33$ and (d) just after the tangency with $b = 1.34$.*

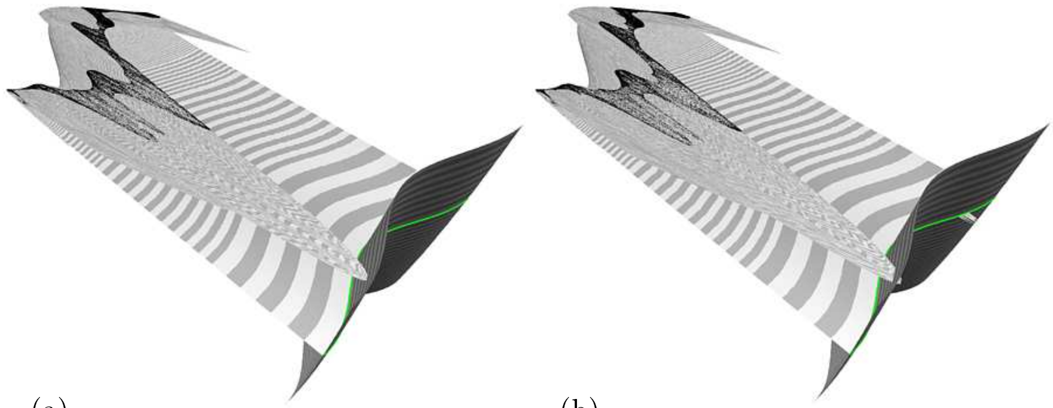

(a) (b)

Figure 6: *When the closures of the stable and unstable manifolds of $H_{\mathcal{B}}$ become tangent for $A = 0.38$ and b in between $b = 1.07$ (a) and $b = 1.08$ (b), a basin boundary metamorphosis happens instead of a boundary crisis.*

Fig. 5; compare also Fig. 4. The manifolds of $H_{\mathcal{B}}$ almost touch each other in Fig. 5(c). The boundary crisis happens at $b \approx 1.334$ due to the homoclinic tangency of the manifolds of $H_{\mathcal{B}}$; for $b = 1.34$ in Fig. 5(d) the stable and unstable manifolds of $H_{\mathcal{B}}$ formed a homoclinic tangle and the attractor is gone.

4.2 When homoclinic tangency and boundary crisis do not coincide

If the homoclinic tangency of the manifolds of $H_{\mathcal{B}}$ does not coincide with the boundary crisis, we expect a basin boundary metamorphosis, as in the unforced case with $c = 0.6$; compare Fig. 2. For $c = 0.1$ without external forcing there is no basin boundary metamorphosis, but we find that a basin boundary metamorphosis exists for certain (nonzero) values of the forcing amplitude A.

Consider the bubble in Fig. 3 in the region $(A, b) \in [0.3, 0.5] \times [0.8, 1.15]$. One would expect that the boundary crisis (BC) curve is a smooth curve, but it has an unexpected irregularity for $A \in [0.3, 0.5]$. In fact, the BC curve continues smoothly for $A \in [0.3, 0.5]$, but then it corresponds to the

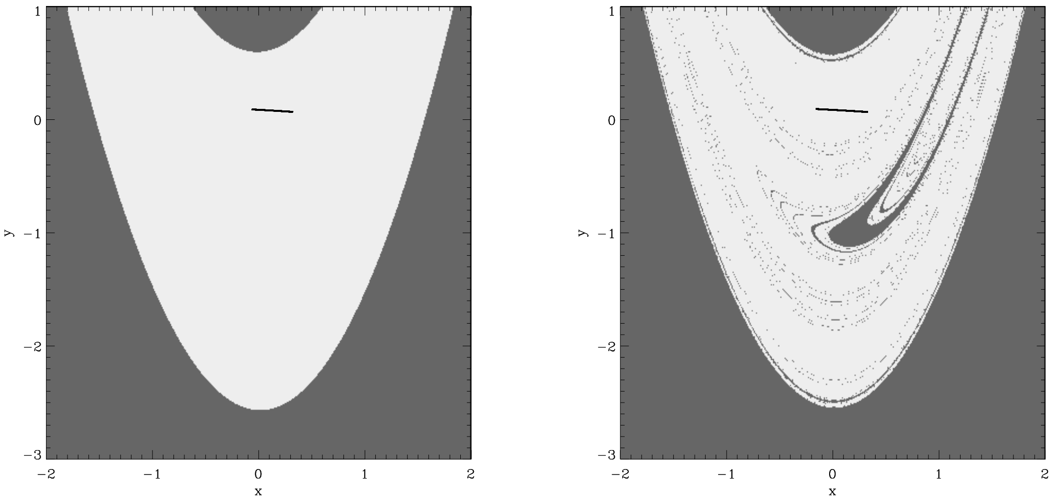

(a) (b)

Figure 7: *Basin boundary metamorphosis for $A = 0.38$. Shown is the basin (white) of the attractor (black) intersected with the plane $\vartheta = 0.25$. The basin becomes fractal for b in between $b = 1.07$ (a) and $b = 1.092$ (b).*

homoclinic tangency of the stable and unstable manifolds of $H_{\mathcal{B}}$. Inside the bubble, the homoclinic tangency of the manifolds of $H_{\mathcal{B}}$ induces a basin boundary metamorphosis as described in [1, 12, 14]. The basin boundary of the attractor suddenly becomes fractal and the relative size of the basin shrinks.

We show this for $A = 0.38$; see Fig. 6 and 7. The attractor changes as b increases, similarly to what happens for $A = 0.2$, and it becomes chaotic for $b \approx 0.976$. Figure 6 shows how the closures of the stable and unstable manifolds of $H_{\mathcal{B}}$ become tangent for b in between $b = 1.07$ (a) and $b = 1.08$ (b). However, the attractor has not grown peaks close to its basin boundary. Hence, for $b = 1.08$ there is homoclinic tangle while the attractor persists. The chaotic attractor disappears in a boundary crisis for $b \approx 1.093$. According to [14], the boundary crisis is then due to a homoclinic tangency of manifolds of a circle with period higher than one, since $H_{\mathcal{B}}$ is no longer accessible. Unfortunately, we were not able to compute this higher periodic circle.

The basin boundary metamorphosis can also be illustrated by computing the basin of the attractor; see Fig. 7. Points that go to the attractor under iteration are plotted white, otherwise they are plotted grey. The attractor is shown in black. Hence, the basin of the attractor is the white region. Figure 7 shows the basin intersected with the plane $\vartheta = 0.25$ for $A = 0.38$, and $b = 1.07$ (a) and $b = 1.092$ (b).

4.3 Two double crisis points

Let us now consider the two end points of the segment on the homoclinic tangency curve where the tangency induces a basin boundary metamorphosis instead of a boundary crisis; see Fig. 8. These points are so-called *double crisis vertices* [9, 22]. The boundary crisis (BC) curve is not differentiable at these points and makes an angle. At the double crisis points a boundary crisis and a basin boundary metamorphosis happen simultaneously. Based on [9, 22], we expect that another bifurcation curve ends at the double crisis vertex, namely a curve of interior crisis related to a sudden change in the size of the attractor. The motivation for this can be understood by comparing Figs. 1 and 2. The relative size of the basin of attraction shrinks a lot after a basin boundary metamorphosis. To avoid a discontinuous jump in the BC curve, the attractor should shrink accordingly, which happens due to a (reversed) interior crisis; see [9].

At the first double crisis vertex, $(A, b) \approx (0.369, 1.090)$, the BC curve makes an angle and the homoclinic tangency of $W^s(H_{\mathcal{B}})$ and $W^u(H_{\mathcal{B}})$ corresponds to a curve of basin boundary metamorphosis. In fact, one can consider the vertex as a point where two different BC curves with two distinct crisis circles end. One of the BC curves, namely the one with $H_{\mathcal{B}}$ as the crisis circle, can be continued smoothly beyond the double crisis vertex as a curve of basin boundary metamorphosis, as it corresponds to the homoclinic tangency of $W^s(H_{\mathcal{B}})$ and $W^u(H_{\mathcal{B}})$. The other curve turns into a curve of *interior crisis* [11, 9, 22]; see Fig. 8. We computed the interior crisis (IC) curve and found that it cannot be continued to small values of A. As the forcing amplitude decreases the attractor becomes less spiky so that it no longer collides with the unstable invariant set that induces the interior crisis. An example of interior crisis is shown in Fig. 9 for $A = 0.35$.

At the second double crisis vertex, $(A, b) \approx (0.474, 0.962)$, the BC curve makes an angle so that it again corresponds to the homoclinic tangency of $W^s(H_{\mathcal{B}})$ and $W^u(H_{\mathcal{B}})$. There is no longer a basin boundary metamorphosis. Again, we expect that an IC curve ends in this vertex [9, 22]. Figure 8 clearly shows this curve as the transition from a nonchaotic attractor to a chaotic

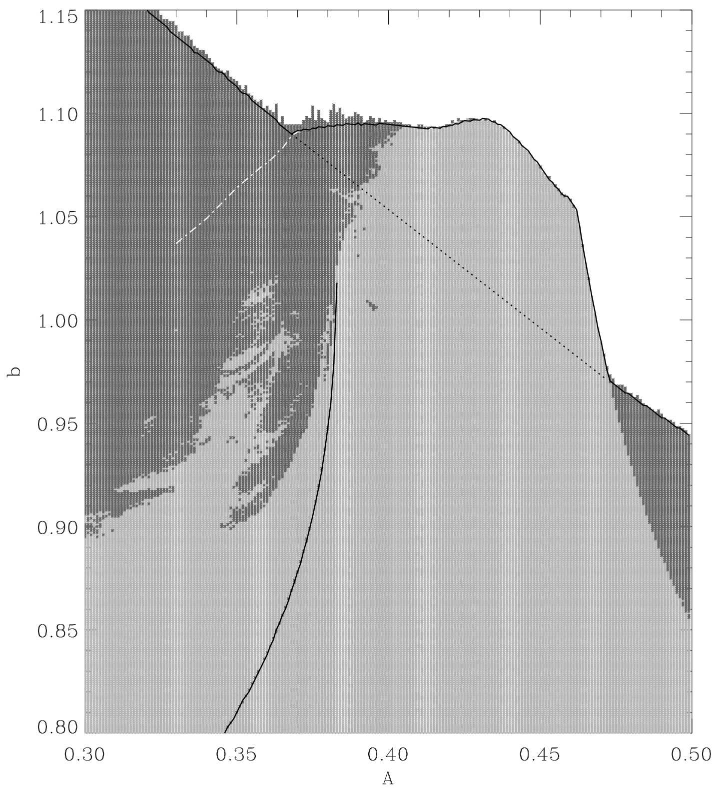

Figure 8: *A detailed bifurcation diagram for the region* $(A, b) \in [0.3, 0.5] \times [0.8, 1.15]$*. Chaotic attractors are dark-gray and nonchaotic attractors light-gray. The solid black curve in the nonchaotic region is the bifurcation curve at which the attractor period-doubles. Also drawn are the curve of basin boundary metamorphosis (dotted black) and the curve of interior crisis that ends at the first double crisis vertex (dashed white).*

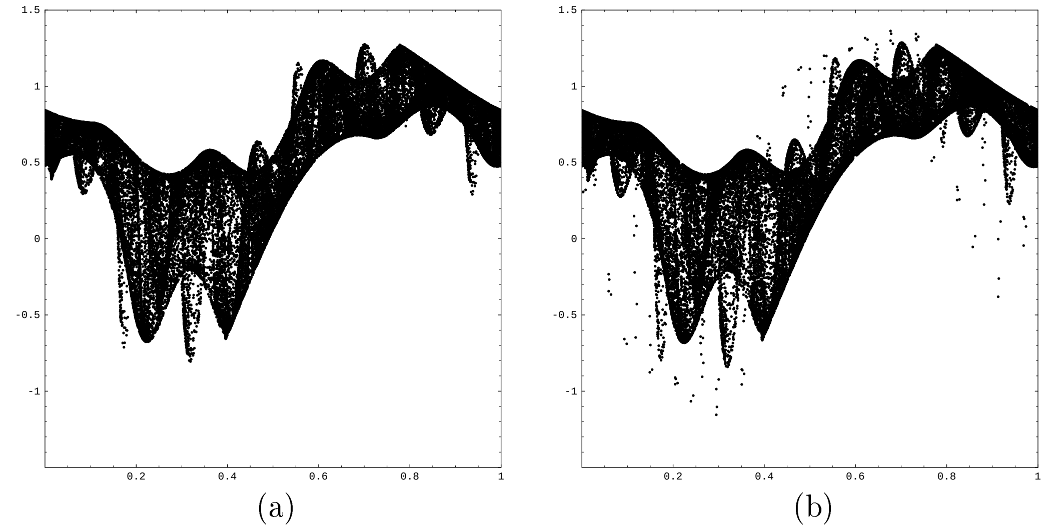

Figure 9: *Interior crisis for* $A = 0.35$*. Notice the difference in size of the attractors for* $b = 1.063$ *(a) and for* $b = 1.064$ *(b), given in the* (ϑ, u)*-projection.*

attractor. This type of interior crisis is visualized in Fig. 10 for $A = 0.48$; compare also [20]. The interior crisis here is essentially different from the interior crisis on the IC curve that ends in the first double crisis vertex. In the latter case the attractor is chaotic both before and after the interior crisis.

5 Discussion

We studied the boundary crisis in quasiperiodically forced two-dimensional dissipative maps using the Hénon map with $c = 0.1$ as a paradigm. The boundary crisis is due to a homoclinic tangency of the stable and unstable manifolds of an invariant (periodic) circle on the basin boundary, called the crisis circle. In most cases this circle is $H_{\mathcal{B}}$, the period-one circle that corresponds to the saddle point $p_{\mathcal{B}}$ of the unforced map. We found that, due to the quasiperiodic forcing, the homoclinic tangency of the manifolds of $H_{\mathcal{B}}$ sometimes induces a basin boundary metamorphosis instead of a boundary crisis. The boundary crisis is then induced by the homoclinic tangency of the manifolds of a higher periodic circle. This implies the existence of double

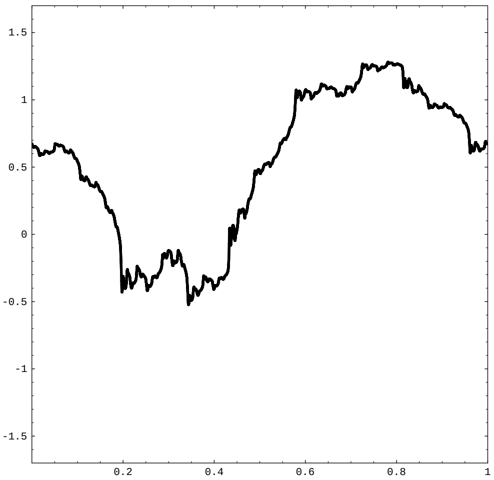

(a)

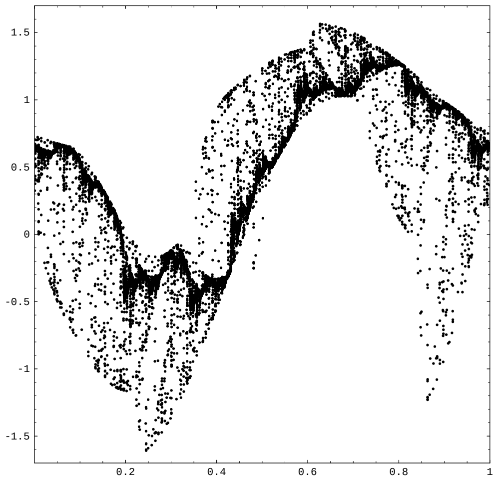

(b)

Figure 10: *Interior crisis for* $A = 0.48$*. Notice the difference in size of the attractors for* $b = 0.9293$ *(a) and for* $b = 0.9294$ *(b), given in the* (ϑ, u)*-projection. Only the attractor for* $b = 0.9293$ *(a) is chaotic.*

crisis vertices, where these two different BC curves and the curve of basin boundary metamorphosis end. As expected [9, 22], we also found the curves of interior crisis that end at those double crisis points.

The double crisis vertices are the beginning and ending of a "bubble" on the BC curve. For A-values in this bubble, the crisis circle has a period higher than one. Unfortunately, we were unable to compute this circle, and hence, we do not know its period. It may be that the period of the crisis circle is changing along the bubble, which would imply that there are more double crisis vertices on the BC curve.

If we were to vary the parameter c, which was kept fixed at 0.1 throughout this paper, the double crisis vertices would change. We conjecture that for certain values of c the two vertices would merge to one. When this happens, the entire homoclinic tangency curve is equal to the BC curve and there is no basin boundary metamorphosis at all. Hence, the BC curve would be differentiable with respect to the (A, b)-plane at this point, but not as a surface in (A, b, c)-space. Such a *multiple crisis vertex* would be characterized as the point on the BC curve where two different IC curves end. Namely, one IC curve is the interior crisis from a chaotic attractor to a chaotic one, and the other IC curve is the interior crisis from a nonchaotic attractor to a chaotic one. The geometric structure of the BC and IC surfaces in (A, b, c)-space is beyond the scope of this paper.

The bubble exists in a neighborhood (in A-values) of the period-doubling curve. If we increase c, we find that we get a second bubble in the neighborhood of the curve where a two-piece attractor period-doubles to a four-piece attractor. This bubble appears to be absent for $c = 0.1$. We expect that extra bubbles appear near the other period-doubling curves as c increases. It is unclear whether the bubble for $c = 0.1$ can disappear for sufficiently small c. The c-value for which a new bubble appears is exactly the point where a multiple crisis point exists.

Acknowledgments

We thank Celso Grebogi for helpful discussions and comments. U.F. acknowledges support from the Deutsche Forschungsgemeinschaft (Heisenberg program and Sfb 555) and thanks the Geometry Center in Minneapolis and the California Institute of Technology for their hospitality and financial support. H.O. is grateful for the hospitality and financial support of the University of Potsdam.

A Numerical methods

Numerical approximations are computed for the attractor, the unstable invariant circle on the basin boundary, and its two-dimensional stable and unstable manifolds. The attractor can easily be computed by iterating arbitrary points in its basin of attraction discarding the initial transient. The invariant circles are of saddle type, which makes it complicated to compute them. Also, since their stable and unstable manifolds are two-dimensional, it is hard to approximate these. In this appendix we summarize how to compute the invariant manifolds.

The computation of an invariant circle of saddle type is based on the graph transform technique described in [18]. The graph transform operator relies on the fact that any point on an approximation of the attractor converges to the real attractor under forward iteration. Similarly, for a repellor one uses backward iteration. If the circle is of saddle type, we can split the space into a subspace where points are attracted to the circle and one where they are expanded from the circle. In the numerical computation, we approximate these subspaces. Then we project the result of a forward graph transform to the attracting subspace, and the result of a backward graph transform to the repelling subspace. The combination of the two projections yields a better approximation of the invariant circle. We refer to [3] for more detailed information.

We remark that the special form of the quasiperiodically forced Hénon map allows for another technique to find the invariant circles. Since the dynamics on the circle is simply the rigid rotation by ω, and since the circle is parametrized in ϑ, we can easily express the invariance of the circle in terms of the parametrization. The resulting equation can then be solved with Newton's method. The advantage of the graph transform method is that it also finds the linear approximation of the stable and unstable manifolds of the circle.

For the computation of the two-dimensional stable and unstable manifolds of the circle, we use the method presented in [19]. The idea is to consider the two-dimensional manifold as a collection of one-dimensional curves in planes defined by $\vartheta =$ constant. Each curve is grown by iteration of the linear manifold near the invariant circle, in such a way that all curves grow with the same speed and in accordance with the local curvature of the manifold.

References

[1] K. Alligood, L. Tedeschini-Lalli, and J. Yorke. Metamorphoses: sudden jumps in basin boundaries. *Commun. Math. Phys.*, **141**:1–8, 1991.

[2] A. Bondeson, E. Ott, and T. M. Antonsen. Quasiperiodically forced damped pendula and Schrödinger equations with quasiperiodic potentials: Implications of their equivalence. *Phys. Rev. Lett.*, **55**:2103–2106, 1985.

[3] H. W. Broer, H. M. Osinga, and G. Vegter. Algorithms for computing normally hyperbolic invariant manifolds. *Z. angew. Math. Phys.*, **48**:480–524, 1997.

[4] P. R. Chastell, P. A. Glendinning, and J. Stark. Locating bifurcations in quasiperiodically forced systems. *Phys. Lett. A*, **200**:17–26, 1995.

[5] P. Collet and J.-P. Eckmann. *Iterated Maps on the Interval as Dynamical Systems*. Birkhauser, 1980.

[6] M. Ding, C. Grebogi, and E. Ott. Evolution of attractors in quasiperiodically forced systems: From quasi periodic to strange nonchaotic to chaotic. *Phys. Rev. A*, **39**:2593–2598, 1989.

[7] W. L. Ditto, M. L. Spano, H. T. Savage, S. N. Rauseo, J. Heagy, and E. Ott. Experimental observation of a strange nonchaotic attractor. *Phys. Rev. Lett.*, **65**:533–536, 1990.

[8] U. Feudel, M. Safonova, J. Kurths, and V. S. Anishchenko. On the destruction of three–dimensional tori. *Int. J. Bifurcation & Chaos*, **6**:1319–1332, 1996.

[9] J. A. C. Gallas, C. Grebogi, and J. A. Yorke. Vertices in parameter space: double crises which destroy chaotic attractors. *Phys. Rev. Letters*, **71**(9):1359–1362, 1993.

[10] C. Grebogi, E. Ott, F. Romeiras, and J. A. Yorke. Critical exponents for crisis-induced intermittency *Phys. Rev. A*, **36**(11):5365–5380, 1987.

[11] C. Grebogi, E. Ott, and J. A. Yorke. Crises, sudden changes in chaotic attractors, and transient chaos. *Physica D*, **7**:181–200, 1983.

[12] C. Grebogi, E. Ott, and J. A. Yorke. Metamorphoses of basin boundaries in nonlinear dynamical systems. *Phys. Rev. Letters*, **56**(10):1011–1014, 1986.

[13] C. Grebogi, E. Ott, and J. A. Yorke. Critical exponent of chaotic transients in nonlinear dynamical systems. *Phys. Rev. Letters*, **57**(11):1284–1287, 1986.

[14] C. Grebogi, E. Ott, and J. A. Yorke. Basin boundary metamorphoses: Changes in accessible boundary orbits. *Physica D*, **24**:243–262, 1987.

[15] G. A. Held and C. Jeffries. Quasiperiodic transitions to chaos of instabilities in an electron-hole plasma excited by AC perturbations at one and at two frequencies. *Phys. Rev. Lett.*, **56**:1183–1186, 1986.

[16] M. Hénon. A two-dimensional mapping with a strange attractor. *Comm. Math. Phys.*, **50**:69–77, 1976.

[17] D.-R. He, W. J. Yeh, and Y. H. Kao. Transition from quasiperiodicity to chaos in a Josephson junction analog. *Phys. Rev. B*, **30**:172–178, 1984.

[18] M. W. Hirsch, C. Pugh, and M. Shub. *Invariant Manifolds*, volume **583** of *Lecture Notes in Mathematics*. Springer, 1977.

[19] B. Krauskopf and H. M. Osinga. Growing 1d and quasi 2d unstable manifolds of maps. *J. Comp. Phys.*, **146**(1):404–419, 1998.

[20] A. Prasad, V. Mehra, and R. Ramaswamy. Intermittency route to strange nonchaotic attractors. *Phys. Rev. Lett.* **79**(21):4127–4130, 1997.

[21] O. Sosnovtseva, U. Feudel, J. Kurths, and A. Pikovsky. Multiband strange nonchaotic attractors in quasiperiodically forced systems. *Phys. Lett. A*, **218**:255–267, 1996.

[22] H. B. Stewart, Y. Ueda, C. Grebogi, and J. A. Yorke. Double crises in two-parameter dynamical systems. *Phys. Rev. Letters*, **75**(13):2478–2481, 1995.

[23] A. Witt, U. Feudel, and A. Pikovsky. Birth of strange nonchaotic attractors due to interior crisis. *Physica D*, **109**:180–190, 1997.

[24] T. Yalcinkaya and Y.-C. Lai. Blowout bifurcation route to strange nonchaotic attractors. *Phys. Rev. Lett.*, **77**:5039–5042, 1996.